Statistical Analysis of Vibration Signals for Monitoring Gear Condition[1]

Moh'd Aqeel Alattas[2] **Moh'd Omer Basaleem[3]**

Abstract

This paper presents a study on the application of vibration signals to detect the presence of defects in gears. Several gear failure prediction methods were investigated and applied to experimental data from a test gear apparatus. The primary objective was to provide a baseline understanding of the prediction methods and to evaluate their diagnostic capabilities. The methods investigated use the signal average in both the time and frequency domain to detect gear failure. Data from eleven gear fatigue tests were recorded at periodic time intervals as the gears were run from initiation to failure. Four major failure modes, consisting of heavy wear, tooth breakage, single pits and distributed pitting were observed among the failed gears. Results show that the prediction methods were able to detect only those gear failures which involved heavy wear or distributed pitting. None of the methods could predict fatigue cracks, which resulted in tooth breakage, or single pits. Additionally, the frequency response between the gear shaft and the transducer was found to significantly affect the vibration signal. The specific frequencies affected were filtered out of the signal average prior to application of the methods.

Keywords : Gears, Failure prediction, Diagnostics

[1] For the paper in Arabic see pages (167 -168).

[2]Associate professor, Mechanical Engineering Dept, Aden University, Aden, Yemen.

[3] Associate professor, Mechanical Engineering Dept, Aden University, Aden, Yemen.

1- INTRODUCTION

There are currently two basic methods of monitoring the condition of drive train components. The first uses a debris monitoring device that detects the size and rate of wear particles in the transmission lubricant as an indicator of severe wear and incipient failure. The second method is based upon vibration data obtained using one or more sensors mounted on the transmission case.

Most debris monitoring devices use magnetically captured debris to detect surface fatigue failures in critical gearbox oil wetted components such as gears and bearings. Some of the debris monitoring devices classify the captured particles by rough sizes, and keep account of the rate of capture and total debris count. This provides an indication as to the damage severity of the failing component(s). One problem with these devices is their limited ability to detect gear failures, since in most cases these-failures do not produce large amounts of metallic debris far enough in advance to provide sufficient warning time [1 ,2, 3,8].

The use of vibration analysis methods for condition monitoring can be further classified into time domain and frequency domain methods. Time domain methods use statistical analysis techniques on direct or filtered time signals to detect parametric or pattern changes as transmission components wear .Statistical methods such as standard deviation and kurtosis are used to qualify general wear from tooth specific damage, respectively. Frequency domain methods use the Fast Fourier Transform (FFT) to convert the time signal into its' corresponding frequency components. Vibration energy at specific frequencies (i.e. primary, harmonics, sidebands, etc.) can be used to monitor gear-train component failures. Both methods use time synchronous averaging to cancel out all vibration that is non-periodic with the shaft frequency being used as the synchronous signal [5 ,6, 7].

This paper is based upon experimental and theoretical work in the area of gear mesh failure diagnostics. More specifically, passive diagnostic instrumentation was installed on a single mesh gear test rig, located at CASM Laboratory at INSA – Lyon (France) to periodically record the gear mesh induced vibration from initiation to failure. This information was analyzed using several existing gear diagnostic methodologies to determine if a correlation exists between the various prediction techniques and the observed modes of failure. This paper presents the

methods used and results obtained when applying the diagnostic techniques to the experimental data.

The analytical work consisted of investigating and applying several gear mesh failure predication techniques. Two of the methods investigated were the FMO and FM4 techniques. FMO is a general method used to detect a variety of failures, whereas FM4 is more sensitive to a single tooth failure such as single tooth fatigue cracks. Also used was the technique utilizing the Hilbert transform to demodulate the time signal. This technique proposed by McFadden [10] is predominately used to detect fatigue cracks early in their development. The remaining three techniques investigated were the crest factor, sideband level ratio, and the non-harmonic to harmonic RMS level energy ratio [4, 11, 16].

The experimental data collected during this work consisted of discrete vibration signatures taken from the eleven gear sets that were run to failure. Two accelerometers, both with a frequency range of 0 to 1000 Hertz, and an optical sensor, used for a shaft synchronous signal, were installed on an existing spur gear test rig. A timer was installed so that the vibration data could be periodically recorded. Of the eleven gear sets monitored, five failed by heavy wear and scoring, two failed by single tooth pitting, two failed by tooth breakage, and two failed by distributed pitting.

2 - THEORY OF GEAR FAILURE PREDICTION METHODS

Several gear failure prediction methods were investigated and applied to the experimental data. The basic theory behind each method is given in the following section:

2.1.) FMO method

The FMO parameter is a time domain discriminate that provides a simple method to detect major changes in the meshing pattern. FMO is written as:

$$FMO = \frac{pp}{\sum_{i=1}^{n} A(f_i)} \qquad (1)$$

where: *pp*- peak-to-peak level of signal average

A - amplitude at mesh frequency (i =1) and harmonics (i > 1).

2.2.) FM4 Method

FM4 was developed to detect changes in the vibration pattern resulting from damage to a single tooth [8,12]. FM4 analysis filters out the regular meshing components from the signal average and performs two statistical operations, standard deviation and kurtosis, on the difference signal. Equation (2) and figure 1 (a, b, c) illustrate the formulation of the difference signal.

$$D(t) = A(t) - R(t) \qquad (2)$$

where:

A(t) - original signal average

R(t) - regular meshing components of signal average

D(t) - difference signal

Figure (1-a) represents a plot of an actual signal A(t) after time synchronous averaging. Figure (1-b) represents a plot of the regular meshing components R(t) of that signal. R(t) is found by taking the FFT of the original signal, extracting the regular components and taking the inverse FFT of these components. The regular components consist of the shaft frequency and its harmonics, the primary meshing frequency and its harmonics along with their first order sidebands. The first order sidebands are generally due to run out of the gear because of machining or assembly inaccuracies [13], and thus are considered regular components. The difference signal is then found by subtracting the regular components from the original signal. Figure (1-c) shows a plot of the resulting difference signal. The FM4 analysis method is comprised of the standard deviation and kurtosis of the difference signal along with a squared representation of the difference signal. The square of the difference signal represented in figure (1- c) is shown in figure (1-d). As seen in this figure the square of the difference signal magnifies any abnormalities present in the difference signal.

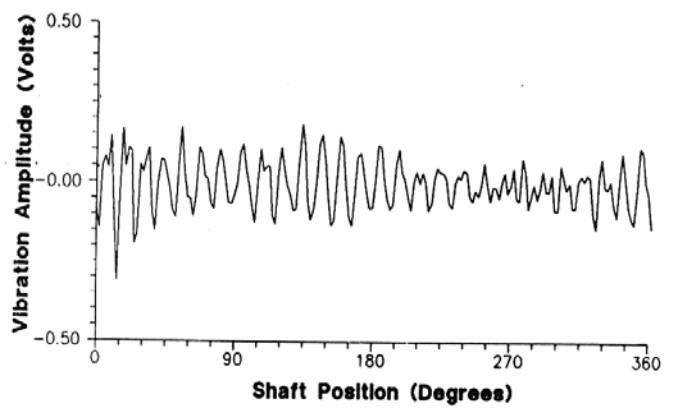

a.) Plot of actual signal average, A(t) for one shaft revolution signal

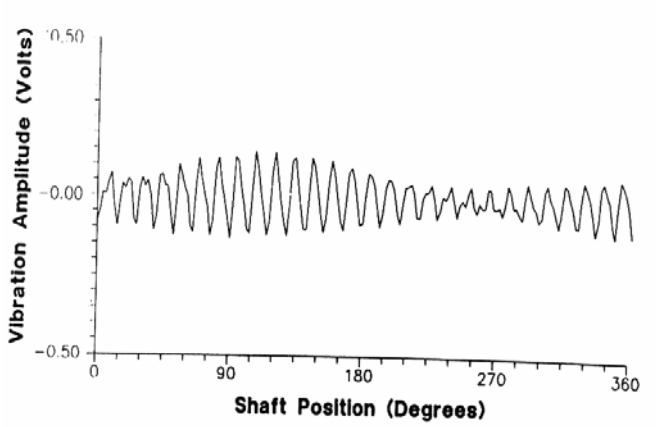

b.) Plot of regular part, R(t), of signal for one shaft revolution

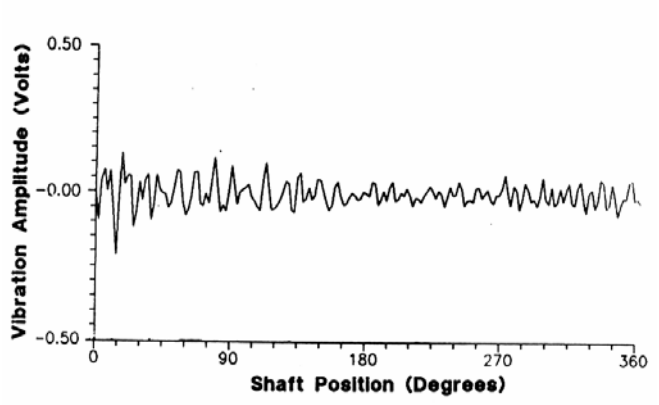

c.) Plot of difference signal, D(t)},
for one shaft revolution

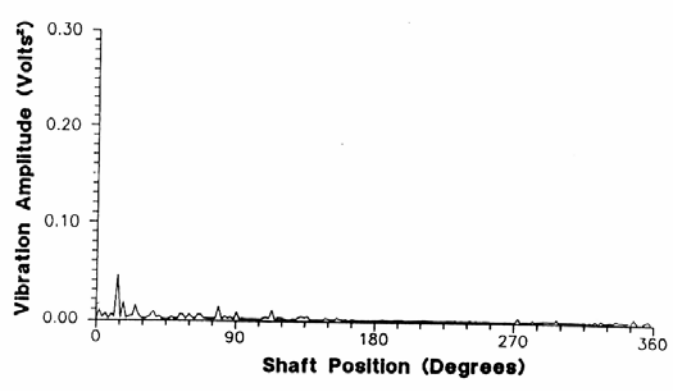

d.) Plot of difference signal, $[D(t)\}^2$,
for one shaft revolution

Fig. (1):Formulation of the difference signal

The FM4 analysis method uses standard deviation and kurtosis to extract information from the resulting difference signal. The standard deviation of the difference signal indicates the amount of energy in the non-meshing components, where the kurtosis indicates the presence of peaks in the difference signal [10, 13, 14].
The standard deviation (RMSDS) of the difference signal can be found using the following equation:

$$RMSDS = \left[\frac{1}{N} \sum_{i=1}^{N} \left(d_i - \bar{d} \right)^2 \right]^{1/2} \qquad (3)$$

where

$\bar{d}$ =Mean value of the signal

Kurtosis (K) is defined as the fourth statistical moment of an array of values about the mean of those values. It is an indicator of the existence of major peaks in the array. The digital form of the kurtosis equation is written as:

$$K = \frac{1}{N} \sum_{i=1}^{N} \left(d_i - \bar{d} \right)^4 \qquad (4)$$

This absolute kurtosis value will increase proportionally with general increases in the standard deviation. To keep the kurtosis parameter sensitive to single tooth damage only, the normalized kurtosis (NK) equation is given below:

$$NK = \frac{N \sum_{i=1}^{N} \left(d_i - \bar{d} \right)^4}{\left[\sum_{i=1}^{N} \left(d_i - \bar{d} \right)^2 \right]^2} \qquad (5)$$

Because the normalized kurtosis values are non-dimensional, signals with different magnitudes but similar shapes will have similar values. A square wave is found to have a normalized kurtosis value of 1.0, for a sine wave the value is 1.5, and for a signal of essentially noise with a Gaussian amplitude distribution the normalized kurtosis value is found to be 3.0. Thus, a normalized kurtosis value greater than 3.0 is indicative of a peak or series of peaks existing in the signal. One pitfall with the normalized kurtosis parameter is its drastic decrease in peak sensitivity as the number of peaks of similar magnitudes increase beyond two. Thus for failures involving two or more teeth, the normalized kurtosis value may not increase far beyond 3.0, and the failure must be detected with the standard deviation level.

2.3.) Hilbert transform method

The basic theory behind this technique is that the sidebands around the dominant meshing frequency modulate the meshing frequency to produce the time average signal. Using the Hilbert transform, the signal can be demodulated, resulting in the corresponding amplitude and phase modulation functions. The phase modulation function is especially sensitive to fatigue cracks by indicating a phase lag at the point the cracked tooth goes into mesh [10].

The Hilbert transform is primarily used to transform a real time signal into a complex time signal with real and imaginary parts. The real part of the complex time signal is the actual time signal, and the imaginary part is the Hilbert transform of the actual time signal. This complex time signal is referred to as the analytic signal (AN), and is given in the following equation.

$$AN(t) = A(t) + iH[A(t)] \qquad (6)$$

where: A(t) = original signal
H[A(t)] = Hilbert transform of original signal

The Hilbert transform of a real valued time signal is defined as the convolution of the time signal with $1/\pi t$, as shown in Equation (7).

$$H[A(t)] = \frac{1}{\pi}\int_{-\infty}^{\infty} A(\tau)\left(\frac{1}{(t-\tau)}\right)d\tau \qquad (7)$$

In order to determine the Hilbert transform of a real-valued time signal, the signal must be transformed to the frequency domain, phase shifted by

-90 degrees, and transformed back to the time domain. Hilbert transform using this method is illustrated in equation (8)

$$H[A(t)] = F^{-1}\left[(-i \operatorname{sgn} f)\, A(f)\right] \quad (8)$$

where: A(f) = Fourier transform of original signal
sgnf = 1 for f > 0 , -1 for f < 0
$F^{-1}[\ ]$ = inverse Fourier transform

Once the analytic signal is found, the amplitude and phase modulation functions can be determined using equation (9).

$$|AN(t)| = \left[(A(t))^2 + (H[A(t)])^2\right]^{1/2} \quad (9)$$

The phase modulation function (ϕ), or instantaneous phase variation. is found by using the following equation:

$$\phi(t) = \tan^{-1}\left[\frac{H[A(t)]}{A(t)}\right] - 2\pi f_0 t \quad (10)$$

Where: f_o = carrier frequency

The phase modulation function, ϕ(t), represents the instantaneous phase angle variation with respect to the nominal gear speed [10, 14]. The second term in equation (10) represents a ramp function with a frequency equal to the carrier frequency, to, that is being modulated. This term is required to separate the instantaneous phase angle variations from the constant carrier frequency phase function.

Before creating the analytic signal, the original signal must be band pass filtered about a dominant meshing frequency. This dominant frequency is either the primary mesh frequency or one of its harmonics, whichever appears to give the most robust group of sidebands. The width of the band pass filter depends on the location of the meshing frequency to other meshing frequency harmonics.

2.4.) Crest factor

The crest factor (CF), is a simple measure of detecting changes in the signal pattern due to impulsive vibration sources, such as tooth breakage [3,9]. The crest factor is easily calculated by dividing the peak level of the signal average to the standard deviation (RMS) of the signal average, as given in equation (11).

$$CF = \frac{Peak\ Level}{RMS} \qquad (11)$$

2.5.) Sideband level factor

The sideband level factor (SLF) is a course indicator of single tooth damage or gear shaft damage [13]. To calculate SLF, the first order sideband levels (FOSL) about the primary meshing frequency are divided by the standard deviation (RMS) of the signal average, as seen in equation (12).

$$SLF = \frac{FOSL}{RMS} \qquad (12)$$

2.6.) Energy ratio

The energy ratio (ER) is formulated to be a robust indicator of heavy uniform wear. This factor divides the standard deviation of the difference signal (RMSDS) by the standard deviation of the signal of the regular components of the signal (RMSRC). Equation (13) illustrates the ER factor.

$$ER = \frac{RMSDS}{RMSRC} \qquad (13)$$

3. EXPERIMENTAL APPARATUS

3.1 TEST RIG

The test rig is a gear simulator constituted of two shafts (1, 2) (Fig. 2), each have 60 mm of diameter and mounted on two bearings. Tested gears are clamped with nuts at the operating end of each shaft and centered by involute splines so as to limit variations of eccentricity. After gear clamping, a special nose is fixed at each shaft end, in order to measure angular positions during motion with optical encoders (C1- C2). The shaft (1) is fixed on a special mounting, made of thick intermediate plates. It permits to impose small misalignments between the two shaft axes. The input shaft (2) is driven by a 120 kW DC motor. The output shaft (1) is braked by a DC motor. Rotating speed is varying between 0 and 10000 rpm and is feedback controlled. The input torque varies independently from 0 to 150 Nm. The active part of the apparatus is fixed on a 7 tons rigid frame (3) made of steel and concrete. An isolating drum (6) permits to decrease the effect of the environment noise.

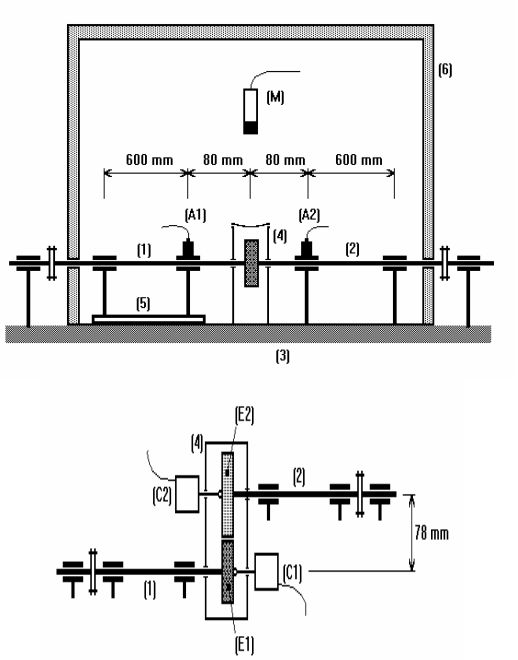

(M) microphone,(A1) and (A2) accelerometers, (C1) and (C2) optical encoders, (E1) and (E2) gears, (1) and (2) shafts, (3) rigid frame, (4) oil box, (5) misalignment plate, (6) isolating case

Fig. 2: Schematic arrangement of the test gear apparatus.

The vibration signal from these accelerometers (A1 and A2) were recorded on a high precision tape recorder, along with a once per revolution signal and a time code signal. A one minute signature was collected every three hours by using a timer to control recording time. The once per revolution signal was provided by a photon sensor that produced a narrow time pulse (0.202 msec) for each revolution of the shaft. This signal was used for time synchronous averaging, and for determining the actual rotational speed. The time code signal was used during tape playback to distinguish between the separate data points, and to provide the exact time and day for each data point recorded.

After the runs were recorded, the data was then analyzed by replaying the tape into a single channel dynamic signal analyzer, with a dynamic range

of 80d8, and transferring it to a personal computer. The raw data was digitized and averaged by the analyzer and sent via a general purpose interface bus to an IBM compatible personal computer. The data transferred was the averaged amplitude and phase portions of the Fourier transform. To apply the various predictive techniques to the experimental data, several computer programs were developed. The programs are written in Fortran . For those methods requiring Fourier analysis, the standard FFT algorithm developed by Cooley and Tukey is included in each routine. The results of the programs are stored in data files that can be plotted using commercially available routines.

3.2 Test gears

The gears tested were all the same type and were subjected to identical loading conditions. All of the gears were made of AISI 9310 steel and were manufactured to AGMA class 13. The test gears have 28 teeth, a pitch diameter of 88.9 mm, a pressure angle of 20 degrees, and a tooth face width of 6.35 mm. The gears were loaded to 74.6 Nm, which resulted in a pitch line maximum hertz stress of 1.71 GPa, at an operating speed of 10,000 rpm. This represents a load of almost two times the normal design load for these gears. This testing procedure was used in order to obtain failures within a reasonable amount of test time. Table (1) lists the basic run parameters along with the number of hours to failure and the overall mode of failure for each run. As seen in this table, the only run parameters that differ between the runs are the surface treatment, and the type of lubricant.

Three different surface treatments were encountered in the eleven runs recorded. The gears in runs 1 through 7 all used the standard surface treatment, which is a final grinding operation to a surface finish of 356 mm rms (14 in. rms). The gears in runs 8 through 11 were shot peened and then honed. The main reason for shot peening is to create subsurface residual stresses that improve the pitting fatigue life of a gear. The gears in runs 8 through 10 used the SPH method, a high intensity shot peening method designed to produce high subsurface residual stresses. The gears in run 11 used the SPL method, a low intensity shot peening method designed to produce low subsurface residual stresses. The basic differences in life and failure modes, as seen in table 1, are primarily due to the different lubricants used.

Table (1): Description of run parameters

Run	Gear surface treatment	Lubrication	Total life (hours)	Basic failure mode
1	Standard	Type A oil	49	Heavy wear and scoring
2	Standard	Type A oil	36	Heavy wear and scoring
3	Standard	Type A oil	9	Broke tooth
4	Standard	Type A oil	79	Heavy wear and scoring
5	Standard	Type A oil	39	Heavy wear and scoring
6	Standard	Type A oil	54	Heavy wear and scoring
7	Standard	Type A oil	50	Broke tooth
8	SPH	Type B oil	520	No failure (single pits)
9	SPH	Type B oil	245	Single pits
10	SPH	Type B oil	339	Distributed pits
11	SPL	Type B oil	200	Distributed pits

The two different oils used were classified type A oil and type B oil. The type A oil did not appear to have sufficient additives to provide a good Elasto-Hydro Dynamic (EHD) film thickness between the gear surfaces under extreme pressure. Without an adequate EHD film thickness, the tooth surfaces obtain metal to metal contact, causing severe surface wear in a relatively short period of time. This is especially evident by the fact that the runs with the type A oil, runs 1 through 7, experienced heavy wear and surface scoring, and an average life of only 63 hours. Comparatively, run 8 through 11, which used oil type B, experienced an average life of 300 hours, and subsurface fatigue failures in the form of pitting. The type B oil was a synthetic paraffinic oil with five volume percent of an extreme-pressure (EP) additive. This EP additive contains sulfur and phosphorus to enable the oil to keep an adequate EHO film thickness, minimizing metal to metal contact, even under extreme pressure.

The failure modes experienced by the various gears can be categorized into four basic damage related groups. These groups are: 1) Heavy wear and scoring, 2) Tooth breakage. 3) Single pits, and 4) Distributed pitting. The groups are based on the types and magnitude of damage found on the gears at the end of their runs. As indicated in table 1, run 8 was not classified as failed because it ran the maximum of 520 hours without exceeding the rig's vibration limit. The point of failure on the fatigue rig

was determined by an overall vibration level from an accelerometer mounted on the rig. When this level reached the preset threshold, the rig shutdown and the run was classified as failed. Because the gears of run 8 experienced damage similar to another run, it is included in that run's group.

4- RESULTS

4.1 FMO-method

The FMO method did very well at detecting a majority of the heavy wear and scoring damage experienced by runs 1, 2, and 4 through 6, as it was designed to do. As seen in figure 3, all of the runs, except run 1, exhibit an increase in the FMO parameter with increasing run time. It is interesting to note that in run 4, the FMO plot indicates heavy damage at 49 hours into the test. Run 1 did not provide good FMO trends even though the gear experienced similar damage.

FMO is designed to detect major tooth faults such as the breakage experienced during runs 3 and 7. Because no data was collected at the time of breakage, or immediately after it occurred, FMO was unable to be applied to these runs.

FMO was applied to runs 8 and 9, which experienced single tooth pits, even though FMO is not designed to detect single tooth faults. As seen in Fig. (3-b), run 8 shows a gradual overall increase in FMO values with run time, and a gradual overall decrease in meshing frequency amplitudes. This trend in run 8 could be attributed to its long run time of 520 hours, which may have resulted in uniform wear not observable by visual inspection. Run 9 showed no logical trend with FMO.

FMO was also applied to runs 10 and 11, where the gears experienced distributed pitting damage. As seen in figure (3-c), the FMO values for both run increase near the end of the run time. Since FMO does not respond to specific tooth damage. It is reasonable to assume that the pitting occurred over enough teeth to act as a uniform wear phenomenon, and thus was capable of being detected by FMO.

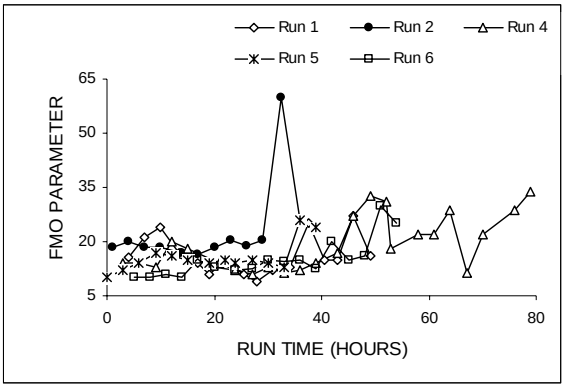

a.) Heavy wear and scoring

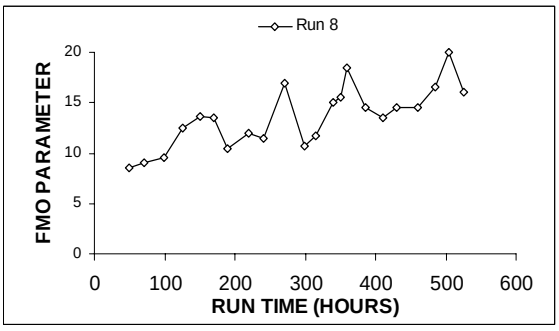

b.) Single pits

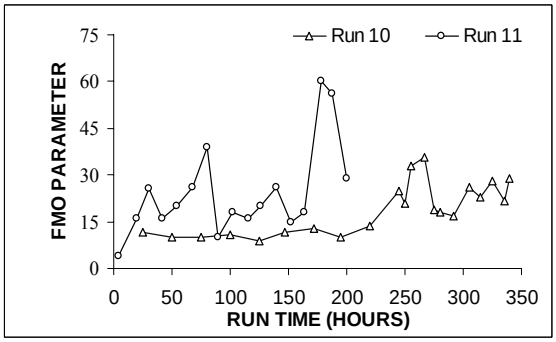

c.) Distributed pits

Fig. (3): Plot of FMO vs run time

4.2. FM4 method

The normalized kurtosis parameter was unable to detect the single tooth faults found in the test gears. Runs 8 and 9 experienced specific faults in the form of one large and one small pit. As seen in figures (4-b) and (4-c), these defects had limited effect on the kurtosis parameter. The fatigue cracks that resulted in broken teeth in runs 3 and 7 were also undetected by the kurtosis parameter, as seen in figure (4-a) for run 7. The normalized kurtosis values for the two data points of run 3, not plotted, were 2.98 and 3.04.

It should be noted that the data points collected at the end of runs 3 and 7 were taken 3 and 2 1/2 hours, respectively, prior to the point of tooth fracture. Only run 11 had limited success using the normalized kurtosis parameter. As seen in figure (4- d), a normalized kurtosis value of 5.3 was registered at 176 hours of operation; however, the value decreased to approximately 3.0 at 192 hours. One explanation for this trend is that only one large pit was present at the 176 hour mark. As more pits forced, the number of peaks increased causing the normalized kurtosis value to decrease.

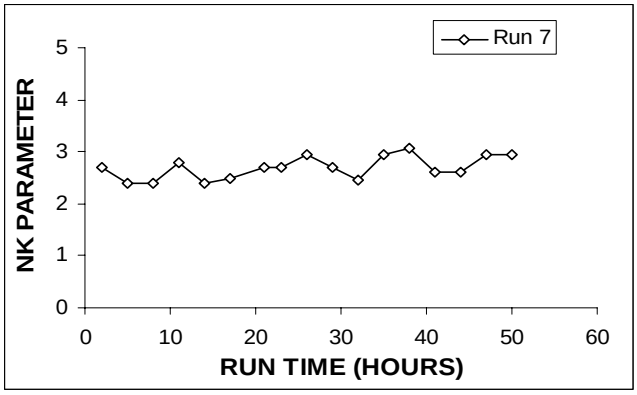

a) Run 7

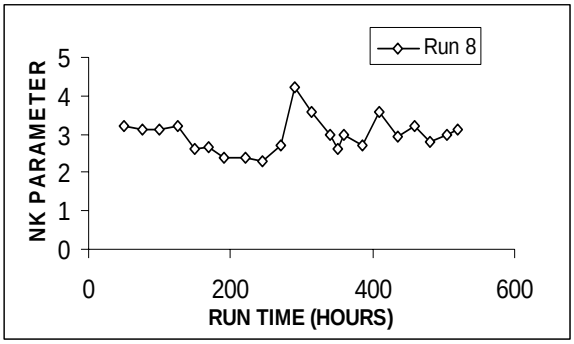

b) Run 8

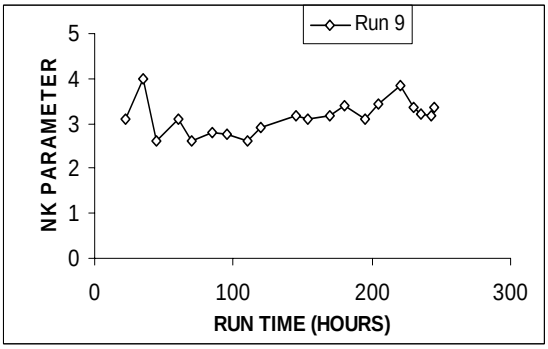

c) Run 9

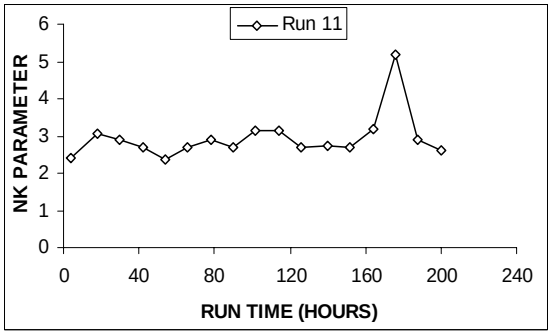

d) Run 11

Fig. (4): Plot of normalized kurtosis vs run time

The standard deviation parameter, although used in FM4 for single tooth failure detection, proved to be a good indicator of heavy wear. Runs 1, 2 and 4 through 6 all experienced heavy wear and scoring. The standard deviation plots for these runs, given in figure (5), all show clear trends of increasing values near the end of each run with only Minor fluctuations. The standard deviation plot of run 1 indicates a definite trend as compared to the FMO plot of run 1, which did not respond to the heavy wear.

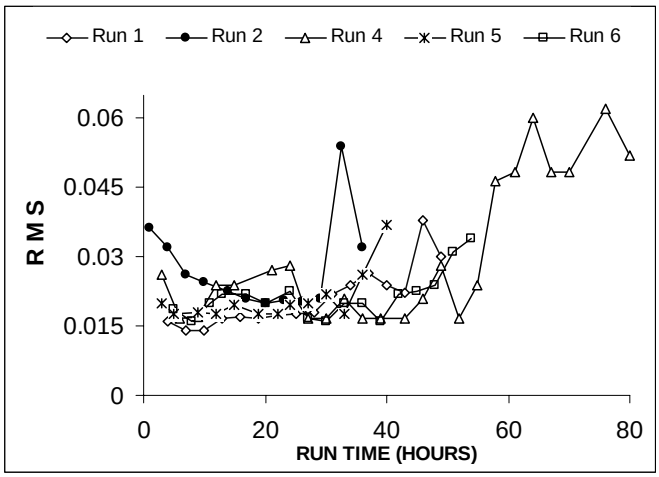

Fig. (5): Plot of standard deviation vs run time

4.3. Hilbert transform method

The Hubert transform method was primarily developed to detect fatigue cracks using the phase modulation function. Runs 3 and 7 are the only runs that experienced tooth fracture due to probable fatigue cracks. Figure 6 plots the phase modulation function for the two data time intervals of run 3.

a.) At a run time of 2 hours

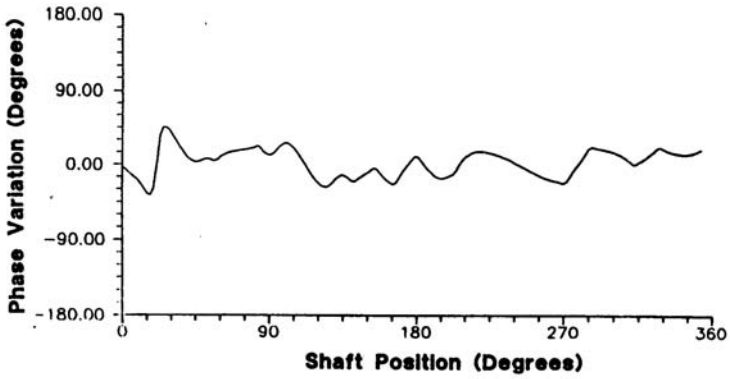

b.) At a run time of 5 hours.

Fig. (6): Plot of phase modulation function for run 3

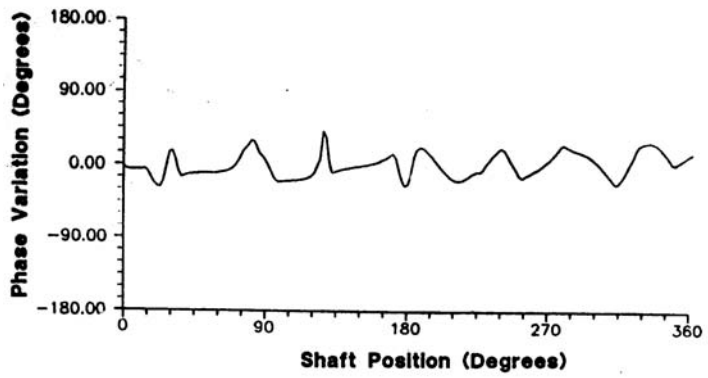

a.) At a run time of 47 hours

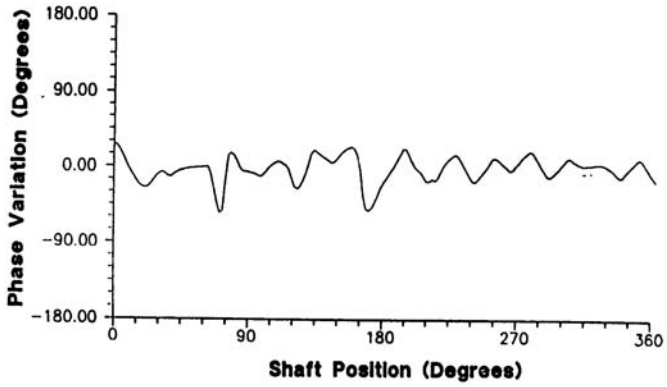

b.) At a run time of 50 hours.

Fig. (7): Plot of phase modulation function for run 7

Several phase shifts can be seen in the first plot. 2 hours into the run; however, they are not reflected in the second plot representing the last data point. Nothing in the last data point plot indicates the presence of a fatigue crack. i.e. no large phase lags present. Figure 7 plots the phase modulation function for the last two data time intervals of run 7. The only possible indication of a fatigue crack starting is the phase lag at approximately half way into the shaft rotation, near the 180 degrees point. The phase lag starts during the second to last time interval, 47 hours into

the run, and grows to the size seen in the last interval, 50 hours into the run. More data after this last data point is required to claim with any certainty that this phase lag represents an actual fatigue crack. Again it must be noted that the last data points for runs 3 and 7 were taken 3 and 2 1/2 hours, respectively, before tooth fracture.

4.4.) Crest factor and sideband level factor

Both the crest factor and sideband level factor are designed to respond to signals with impulsive vibration sources, specifically tooth breakage. Runs 3 and 7 were the only runs that experienced tooth fracture. The crest factor and sideband level factor for run 7 are plotted in figure 8. Run 3 was not plotted, since it had only two time intervals recorded before fracture occurred. As seen in figure 8, neither the crest factor (plot a) or the sideband level factor (plot b) display any indication that a tooth fracture was going to occur. These parameters may be sensitive to tooth breakage only after it has happened. Unfortunately, no data was collected during or after the fracture occurred.

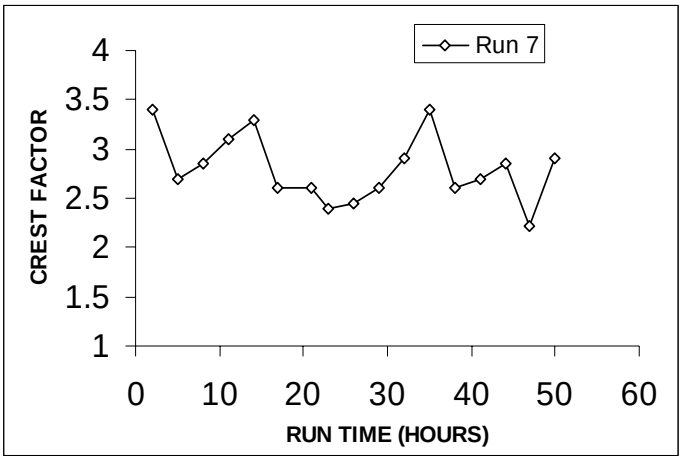

a.) crest factor

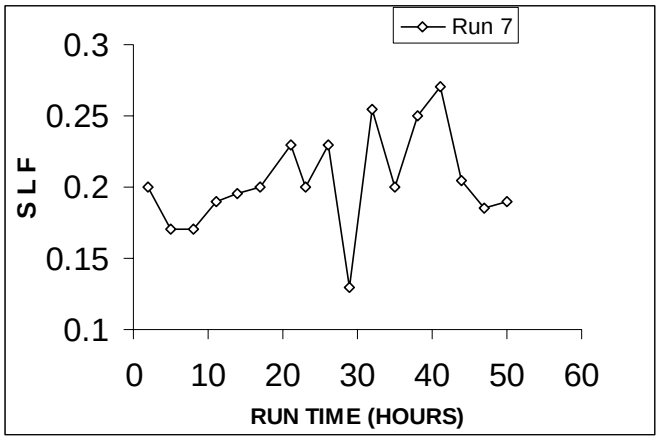

b.) sideband level factor

Fig. (8): Plot of crest factor and sideband level vs run time for run 7

4.5. Energy ratio

The energy ratio is designed to be a robust indicator of heavy wear. Runs 1, 2, and 4 through 6 experienced heavy wear and scoring. The energy ratio graphs of these runs are given in Fig. (9 – a). As seen in this figure, the energy ratio does not provide as good an indication of wear as the FMO and the standard deviation methods. The energy ratio graphs for runs 10 and 11 are given in Fig. (9 – b). Of these two runs, only run 10 had an increase in its energy ratio parameter.

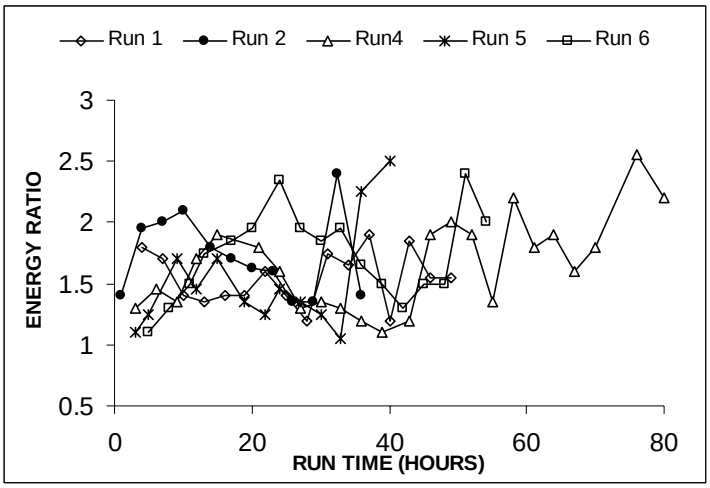

a.) Heavy wear and scoring (Run 1,2,4,5 and 6)

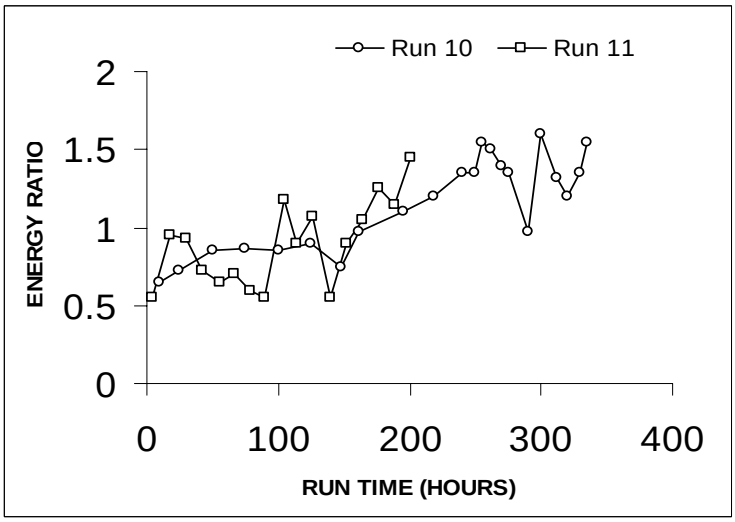

b.) Distributed pits (Run10 and 11)

Fig. (9): Plot of energy ratio vs run time

5 - CONCLUSIONS

The type and extent of the damage found on the eleven test gears can be classified into four Major failure modes. The first mode can be described as heavy wear and scoring (runs 1,2 and 4 through 6). The second mode is tooth breakage (runs 3 and 7). The third failure mode is a result of single pits (runs 8 and 9). And the last mode is described as distributed pitting (runs 10 and 11). These classifications will be used to evaluate the overall performance of the various methods.

1. Heavy wear and scoring

The FMO parameter and the standard deviation of the difference signal from FM4 did very well at detecting this heavy wear condition. Results from both techniques support the theory that as a gear wears the meshing energy redistributes from the meshing frequencies to its sidebands and beyond.

The energy ratio method does not predict wear as well as the FMO and the standard deviation methods. The most probable reason for this is in the denominator of the energy ratio. The denominator is the standard deviation of the regular signal, or the meshing frequencies and their first order sidebands. The first order sidebands should not be considered part of the regular signal for this parameter. This is because they increase in amplitude similar to the higher order sidebands as the gear wears.

An enhanced method using a combination of these techniques could prove to be a reliable uniform gear wear detection technique. One such method could use the standard deviation of the difference signal divided by the sum of the amplitudes of the meshing frequencies (primary and first harmonic). Because wear becomes detectable in the overall vibration level only when it reaches a critical stage, a robust wear indication parameter would be highly useful.

2. Tooth breakage

The fatigue cracks that resulted in the broken teeth in runs 3 and 7 were not detected by any of the methods. The normalized kurtosis parameter of FM4، the phase modulation function from the Hilbert transform technique, the crest factor, and the sideband level factor are all conditioned to react to tooth cracks to varying degrees; however, none detected any fault prior to tooth fracture. The most probable reason for this can be due to the high speed and high loading conditions the test gears are subjected to. With these operating conditions, the time elapsed

between initiation of the fatigue crack and eventual tooth fracture is probably orders of magnitude lower than the three hour data interval time. Since the last time records collected from runs 3 and 7 were 3 and 2 1/2 hours before actual tooth fracture, respectively, data necessary to indicate the fatigue cracks were missed.

3. Single pits

The single pits were not detected by the normalized kurtosis in the FM4 technique. The normalized kurtosis of the difference signal is designed to detect tooth specific faults; however, no indication of these defects were recorded with this parameter. Although they physically appear large, they may have not affected the signal to the point detectable by FM4.

4. Distributed pitting

The distributed pitting damage was detected with the FMO parameter. It is theorized that the pitting happened over enough of the teeth to act as a uniform wear phenomenon, thus becoming detectable to FMO. The square of difference signal from the FM4 method did appear to reflect the actual wear pattern on some of the runs.

6 – REFEERENCES

1.) Al-Attass, M., Mahfoudh, J., Remond, D. and Play, D., 1994, " Experimental Study of Faults Influence on Vibration and Noise Measurements in Gear Transmission Mechanism." 1994 Gearing International Conference , Newcastle, pp. 469 - 474.

2.) Al- Attass, M., Mahfoudh, J. and Play, D., 1994, " Vibration Analysis for Detection of Gear Faults Within Gearbox: Application to Spur and Helical Gears, Fourth International Conference on Rotor Dynamics, IFToMM, Vibration Institute, Chicago, pp 197-205

3.) Al- Attass, M., Mahfoudh, J. and Play, D., 1996, "Morphological Study of Vibratory Signals: Identification of Spur and Helical Gear Faults" Revue française de mécanique, N°1, pp. 33- 40.France

4.) Alloud, J.P., 1978, " L'analyse Statistique Dynamique Appliquée à la Maintenance Préventive des Machines Tournantes" J. Mécanique-Matériaux-Electricité, N° 341-342, pp. 276-281. France.

5.) Droiche, K., Sidahmed, M. and Garnier, Y., 1992, "Détection de Défaut d'Engrenage par Analyse Vibratoire", J. Traitement du signal , Vol. 8, N° 5, pp. 331-343. France.

6.) Drosjack, M. J. and Houser, D. R., 1977, " An Experimental and Theoretical Study of the Effect of Simulated Pitch Line Pitting on the Vibration of a Geared System", ASME 77-DET 123, 11P.
7.) Mahfoudh, J., Bard, C,. Al- Attass, M. and Play, D.,1995," Simulation of Gearbox Dynamic Behaviour with Gear Faults" Second International Conference on Gearbox Noise, Vibration and Diagnostics, IMECH, London, pp. 91-100.
8.) Mathew, J., 1989, " Monitoring the Vibrations of Rotating Machine Elements- An Overview", The 1989 ASME Design Technical Conference on Mechanical Vibration and Noise, Montreal- Canada, pp 15-22.
9.) Mathew, J. and Alfredson, R. J., 1984, "The Condition Monitoring of Rolling Element Bearing Analysis" J. Vibration, Acoustic, Stress, and reliability design, Vol. 106, pp. 447 - 453.
10.) McFadden, P. D., 1985, " Low Frequency Vibration Generated by Tooth Impacts." NDT International, Vol. 18, N° 5, pp. 279-282.
11.) Monk, R., 1979 " Machine Health Monitoring - Some Common Defects." J. Noise Control Vibration , Vol. 10, N° 1, pp. 24-26.
12.) P. Gadd, " Condition Monitoring of Helicopter Gearboxes Using Vibration Analysis Techniques" , 1984, AGARD conference proceedings, No. 369, Lisbon.
13.) Randall, R. B., 1982, "A New method of Modelling Gear Faults", ASME, J. Mechanical Design, 104, pp 259-267.
14.) Stewart, R. M., 1980, "The Specification and Development of a Standard for Gearbox Monitoring", Proc. Instr. Mech. Eng., pp 353-358.
15.) A. VanDyck, G. Cotterill, 2005,"Improved Machine Condition Monitoring", Maintenance Journal, Vol. 18 No. 2. Australia.
16.) Walsh, C. T., 1992 " Condition Monitoring of Machine Systems for the 1990 s and Beyond." J. Machine vibration, vol. 1, pp. 203-210.

Received, 30 May, 2006.